Journal of Materials Chemistry C

PAPER

View Article Online
View Journal | View Issue

Cite this: J. Mater. Chem. C, 2016, 4, 2886

Multiresponsive luminescent dicyanodistyrylbenzenes and their photochemistry in solution and in bulk†

M. Martínez-Abadía,[a] S. Varghese,‡[b] R. Giménez*[a] and M. B. Ros*[a]

Received 10th September 2015,
Accepted 2nd November 2015

DOI: 10.1039/c5tc02852c

www.rsc.org/MaterialsC

Multiresponsive luminescent materials with dicyanodistyrylbenzene chromophores incorporated into bent-core and rod-like molecules have been prepared and characterized. Rod-like compounds exhibit nematic or smectic liquid crystal phases, whereas bent-core compounds melt directly to the isotropic liquid at high temperatures. Fluorescence properties are very sensitive to external stimuli such as heat, light, pressure and solvent vapors. All compounds undergo *Z*/*E* photoisomerization in solution under UV irradiation. In addition, photochemical activity in bulk has been investigated. Whereas the crystal phases are stable under UV irradiation, the liquid crystal phases are unstable giving rise to *Z*/*E* photoisomerization and [2+2]-photocycloaddition products. As a consequence, photoinduced phase changes are observed. This study shows the versatilty of dicyanodistyrylbenzene-based liquid crystals as novel types of photoreactive materials.

Introduction

The dicyanodistyrylbenzene (DCS) unit is a π-conjugated platform with interesting optical properties such as tuneable luminescence emission in the visible spectra and aggregation induced enhancement in emission (AIEE) properties.[1–3] Photoluminescence emission occurs at higher wavelengths compared to their homologous α-cyanostilbenes,[4,5] as a consequence of their longer conjugation length. In addition, DCS and its derivatives exhibit interesting material properties such as multistimuli luminescence switching,[6–13] two-photon absorption,[14] lasing[15–21] and liquid crystal behavior,[6,11,20,22,23] evolving as a chromophore with broad optoelectronic applicability. Although it is known that α-cyanostilbenes can give rise to *Z*/*E* isomerization or [2+2]-cycloaddition reactions in solution, monolayers or in bulk,[24–36] the photochemistry of DCS compounds has been barely studied, being only reported in solution.[37–39]

While continuing our interest in the study of cyanostilbene-based chromophores and their different supramolecular organization in the bulk, we are interested in liquid crystal phases such as the non-conventional bent-core mesophases[40,41] as a way to obtain novel soft materials with multiresponsive properties. Herein we report the synthesis and characterization, as well as the liquid crystal properties and the photophysical and photochemical properties of bent-core molecules and rod-like molecules with DCS chromophores. Three novel bent-core structures, **B14-DCS14**, **B14-DCS4** and **B4-DCS4**, with different alkoxy terminal substituents (*n*-tetradecyloxy or *n*-butoxy) were prepared (Fig. 1) and their thermal and optical properties were investigated.

Interestingly the synthetic route offered two rod-like dicyanodistyrylbenzene derivatives (**DSC14** and **DCS4**) as by-products (Fig. 1), which gave us the possibility to broaden our understanding of the influence of incorporating DCS chromophores into a 2D *versus* a 1D molecular geometry.

DCS4 has been reported.[7,13] However, novel properties that have not been previously described such as liquid crystal behavior and photochemical activity are stated here.

Apart from the fluorescence properties, we demonstrate that the DCS unit is photoreactive in solution and some condensed phases, giving rise to photoproducts from *Z*/*E* isomerization and [2+2]-cycloaddition reactions upon irradiation, similar to that reported for α-cyanostilbenes. This significantly alters the material properties such as phase transition temperatures and optical properties. Therefore, their photochemical activity is an important issue to be taken into account when preparing and manipulating DCS based compounds. Aspects related to the synthesis, purification and investigation of their optical/photophysical properties should be carefully undertaken in

[a] Instituto de Ciencia de Materiales de Aragón (ICMA), Departamento de Química Orgánica-Facultad de Ciencias, Universidad de Zaragoza-CSIC, 50009 Zaragoza, Spain. E-mail: rgimenez@unizar.es, bros@unizar.es
[b] Instituto Madrileño de Estudios Avanzados en Nanociencia (IMDEA Nanociencia), Ciudad Universitaria de Cantoblanco, E-28049, Madrid, Spain

† Electronic supplementary information (ESI) available: Synthesis and characterization data, DSC thermograms, POM pictures of the mesophases, XRD, TGA and UV-Vis and luminescence spectra. See DOI: 10.1039/c5tc02852c

‡ Current address: School of Physics and Astronomy, University of St Andrews, UK.

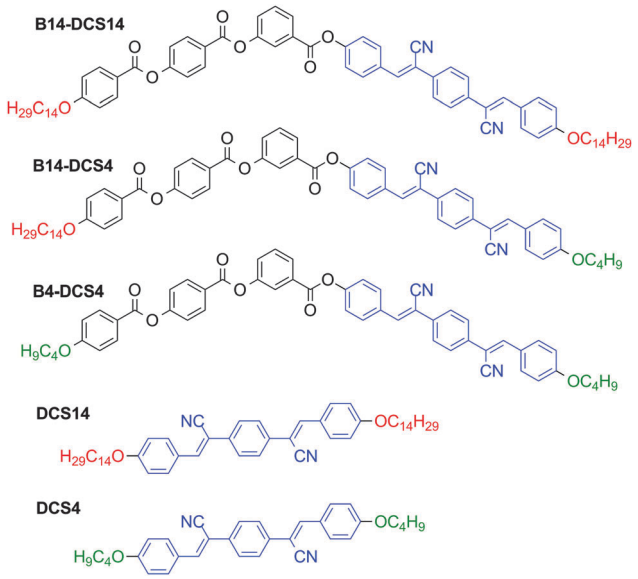

Fig. 1 Chemical structures of the DCS derivatives studied in this work.

order to obtain reproducible results and future implementation in devices based on these chromophores.

Results and discussion

Synthesis and characterization

The synthetic route (Scheme 1) starts with a Knoevenagel condensation of 1,4-phenylenediacetonitrile with two moles of *p*-hydroxybenzaldehyde, giving compound **1**[42] with 87% yield. Compound **1** was then alkylated with 1-bromotetradecane or 1-bromobutane to yield monoalkylated compounds **2** and **3**, which were esterified with acid chlorides derived from benzoic acids **7** and **8** (the synthesis is reported in the ESI†) to yield the final bent-core compounds **B14-DCS14**, **B14-DCS4** and **B4-DCS4**. The rod-like compounds **DCS14** and **DCS4** were obtained as by-products from the monoalkylation reaction of compound **1** with 1-bromotetradecane or 1-bromobutane, respectively, although the reaction was fed with a stoichoimetric defect of alkyl bromide (0.8 mol of alkyl bromide per mol of **1**).

The chemical structures were confirmed by NMR, FTIR, MS and elemental analysis (see ESI†). In all cases the compounds were obtained with a *Z* configuration for both the C=C double bonds of the DCS unit (*Z*,*Z* isomer), as drawn in Fig. 1.

Care was taken to avoid exposure to ambient light during the synthesis and purification in order to prevent *Z*/*E* photoisomerization. As is explained below, in the photochemical section, this photoreaction takes place when the compounds are in solution. On the other hand, any possible isomerization products formed during these steps can be reverted to the *Z*,*Z* isomer by recrystallization in ethyl acetate.

Thermal properties

The thermal and liquid crystalline properties were studied using a polarized optical microscope equipped with a Linkam hot stage and a 450 nm longpass filter. The filter was necessary to avoid photochemical reactions that vary the composition, and therefore the phase transition temperatures. In addition, thermogravimetric analysis (TGA) and differential thermal calorimetry (DSC) were performed. The phase transition temperatures and the corresponding changes in enthalpy are collected in Table 1.

Bent-core compounds do not exhibit liquid crystalline behavior and melt directly to an isotropic liquid phase. Melting points are always higher than 195 °C even for the *n*-tetradecyloxy substituted compounds, much higher than previously reported bent-core cyanostilbenes.[40] This is a consequence of the combination of

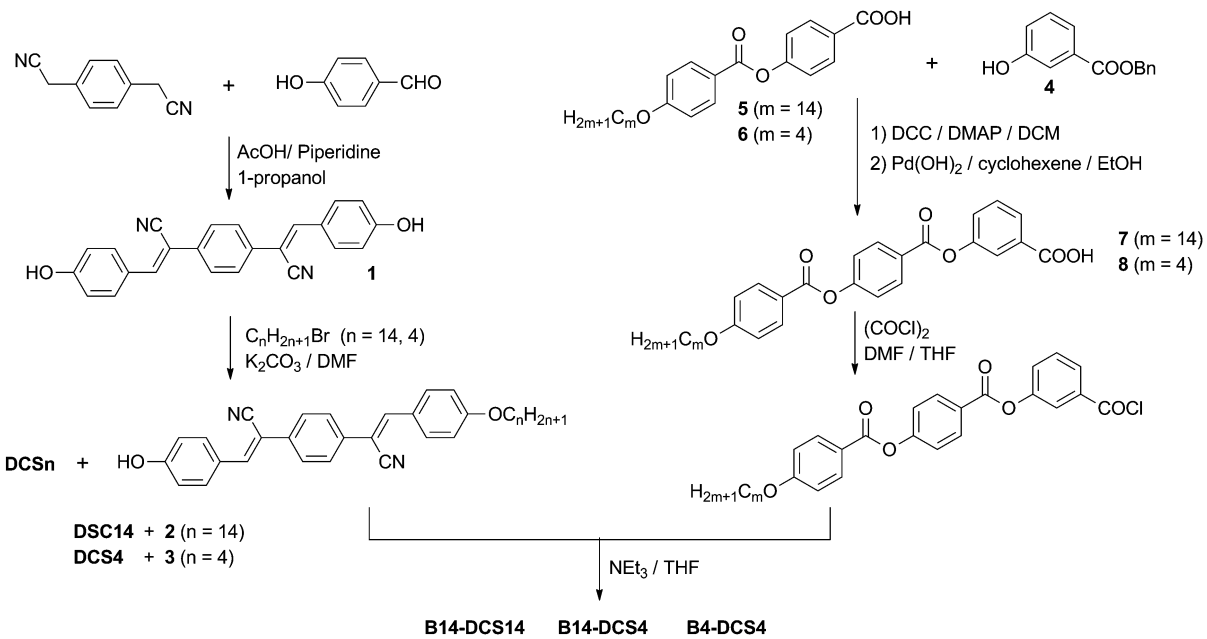

Scheme 1 Synthetic strategy followed for the preparation of DCS derivatives.

Table 1 Thermal and liquid crystalline properties of DCS derivatives

Compound	Phase transition[a,b] T/°C (ΔH/kJ mol^{-1})
B14-DCS14	Cr 195 (48.8) I
	I 185 (49.3) Cr
B14-DCS4	Cr 211 (51.7)[c] I
	I 185 (51.1) Cr
B4-DCS4	Cr 216 (47.4) I
	I 208 (44.9) Cr
DCS14	Cr 122 (49.5) SmC 194 (10.8) I
	I 193 (10.5) SmC 105 (49.2) Cr
DCS4	Cr 174 (30.1) N 242 (0.9) I
	I 239 (1.0) 164 (0.3) SmC 161 (21.3) Cr

[a] Data determined by DSC, temperatures at the maximum of the peaks from the first heating and cooling cycle at a scanning rate of 10 °C min^{-1}. Cr: crystal phase, I: isotropic liquid phase, SmC: smectic C mesophase, N: nematic mesophase. [b] The crystal phase denoted as Cr, in most cases, is not unique and crystalline polymorphism is observed (see thermograms in the ESI). [c] Combined enthalpy of two crystalline transitions.

several effects, primarily the central 1,3-benzoic ring is known to increase the melting point of bent-core compounds compared with analogous 1,3-phenylenes or 3,4-biphenylenes.[43]

Secondly, as the main factor, the presence of the long conjugated DCS unit as a lateral part of the bent-core structure. The combination of both these effects induces strong intermolecular interactions that prevent the formation of mesophases, favoring the stabilization of crystalline phases.

However, rod-like compounds are both liquid crystalline. **DCS14** displays a rich crystal polymorphism and a smectic C mesophase (SmC) for a wide temperature range of 70 °C, identified by *Schlieren* and broken fan-shaped textures at POM (Fig. S6b, ESI†). This mesophase has been further confirmed by XRD (Fig. S7a, ESI†). A diffuse halo at wide angles typical of a fluid phase is observed, together with a reflection in the low-angle region at a distance of 37.9 Å. This value is much smaller than the calculated molecular length (57 Å), indicating that the molecules are tilted inside the layers.

Compound **DCS4** shows higher transition temperatures and displays an enantiotropic nematic mesophase (N) with a *Schlieren* texture (Fig. S6d, ESI†). In the cooling process a monotropic SmC mesophase also appears below the N phase just before crystallization takes place. The N phase was also confirmed by XRD (Fig. S7b, ESI†), since the diffractogram shows two diffuse haloes characteristic of this phase.

A common tendency of rod-like liquid crystalline materials is also found here, molecules with short alkoxy chains favour nematic mesophases while long alkyl chains favour smectic phases. In the same line as here, a similar rod-like DCS compound with *n*-dodecyloxy chains has also been reported to exhibit a smectic liquid crystalline phase.[11]

Photophysical properties

The UV-Vis absorption and fluorescence spectra of all these derivatives were recorded in dichloromethane (DCM) solutions (Table 2). Bent-core compounds show two absorption bands in DCM at around 270 and 372 nm, corresponding to the polybenzoate structure and the DCS chromophore, respectively. They show weak luminescence, with an emission maximum at around 455 nm. The low luminescence yield of DCS-based molecules in dilute solution is attributed to non-radiative decay paths associated with torsional modes.[3] In diluted PMMA films (solid solutions) of these compounds the emission wavelengths shift to the blue and the quantum yields increase by one order of magnitude. This effect has been previously observed in α-cyanostilbenes[41] and it is a consequence of the rigid environment, which hinders the non-radiative deactivation pathway through torsional modes.

The fluorescence emission behavior of the bent-core molecules has also been studied in the as-obtained solids (Cr_1) (Table 2). The emission bands appear at much higher wavelengths (573–588 nm) compared to solution, giving rise to an orange emission. The quantum yields are higher than in solution, being similar to PMMA solutions, about 4–6%. The average fluorescence lifetime was observed in the range of 10.2 to 14.2 ns. In the powder (Cr_1), the non-radiative rate is found to be an order of magnitude higher than that of the radiative rates. This is in stark contrast to the rod shaped molecules, where the radiative rates have a slight upper hand over the non radiative rates, which makes the rod-like molecules reasonably emissive.[3,44,45] The reason for the low radiative rates in the bent shaped molecules is not very clear and should be related to the common 'bent-core bunch' packing features of bent-core molecules that give rise to different degrees of H-aggregation.[41]

It is interesting to note that the emission, albeit weak, does not only change from liquid or solid solutions to the bulk, but it is also sensitive to different thermal processing of the bulk solid (thermochromism), as a consequence of inducing different

Table 2 UV-Vis and fluorescence data in dichloromethane (DCM) solution, dissolved in PMMA and in the as-obtained solid[a]

	DCM				PMMA		As-obtained solid (Cr_1)				
Compound	λ_{abs}/nm	$\varepsilon/10^4$ L mol^{-1} cm^{-1}	λ_{em}/nm	Φ_F[b] (%)	λ_{em}/nm	Φ_F[c] (%)	λ_{em}/nm	Φ_F[c] (%)	τ_F/ns	k_r[d]/s^{-1}	k_{nr}[d]/s^{-1}
B14-DCS14	269, 372	3.6, 4.6	453	0.20	445	4.0	588	6.0	14.15	4.2×10^6	6.6×10^7
B14-DCS4	272, 372	3.9, 5.3	453	0.20	439	3.0	573	4.0	10.17	3.9×10^6	9.4×10^7
B4-DCS4	271, 371	3.8, 5.5	455	0.20	440	4.0	586	5.0	10.70	4.7×10^6	8.9×10^7
DCS14	381	5.9	449	0.20	434	13.0	564	53.0	17.07	3.1×10^7	2.8×10^7
DCS4	381	5.9	448	0.30	434	12.8	517	56.1	6.59	8.5×10^7	6.7×10^7

[a] Absorption and emission maxima (λ_{abs}, λ_{em}), fluorescence quantum yields (Φ_F), lifetimes (τ_F), radiative and non-radiative rates (k_r, k_{nr}). [b] From relative measurements using 9,10-diphenylanthracene in cyclohexane as a reference (Φ_F = 0.9). [c] From absolute measurements in an integrating sphere. [d] From $\tau_F = 1/(k_r + k_{nr})$, $\Phi_F = k_r \cdot \tau_F$.

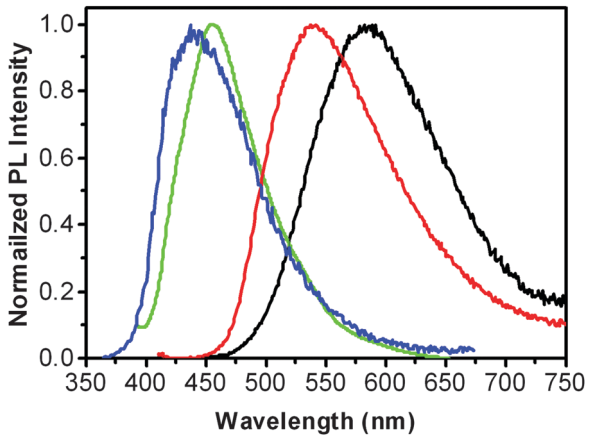

Fig. 2 Fluorescence spectra of **B4-DCS4** in DCM solution (green), PMMA (blue), as-obtained solid (black) and processed solid (red).

molecular packing. For all bent-core compounds the emission of the as-obtained solid (Cr_1) is different from the emission of a processed solid obtained by heating the compound up to the isotropic liquid, then cooling down at 10 °C min^{-1} to r.t. and measuring it after 24 hours. The differences range up to a 40 nm blue-shift of the emission band. Fig. 2 illustrates this property for compound **B4-DCS4**, showing the different emissions in DCM solution (455 nm), PMMA films (440 nm), the as-obtained solid (586 nm) and the processed solid (540 nm).

The UV-Vis absorption and emission spectra of the rod-like compounds in solution are in agreement with those previously reported for similar compounds, with absorption maxima at 381 nm and emission at 448 nm, slightly different from the DCS bent-core compounds as a consequence of the different substitution at the ends of the DCS chromophore (alkoxy/alkoxy *vs.* oxycarbonyl/alkoxy).

The luminescence of the rod-like compounds is very sensitive to environmental changes, exhibiting thermo-, mechano- and vapochromic properties. This multiresponse property has been previously reported for compound **DCS4**,[7] and for a similar analogue with *n*-dodecyloxy terminal chains.[11] An in-depth study attributes the origin of the multiresponsive behavior to the ability of this compound to easily change between crystal phases with different π-stacking, due to the shear-sliding capability of molecular sheets *via* external stimuli, driven by different modes of local dipole coupling.[7]

The new rod-like compound **DCS14** also exhibits multiresponsive behavior, showing broad color changes ranging from orange to blue (Fig. 3) with multiple external stimuli. The as-obtained powder (Cr_1) is orange in color and shows an orange luminescence under irradiation with a 365 nm UV lamp. The orange luminescence shifts to green after thermal processing that consists of heating up to the liquid crystal phase at 185 °C and cooling down to room temperature (Fig. 3A). The DSC thermogram clearly shows that the processed solid is different from Cr_1 (Fig. S6a, ESI†). Quite interestingly, and as a consequence of the rich polymorphism, a different thermal processing yields a much blue shifted emission. Heating as-obtained powder (Cr_1) for one

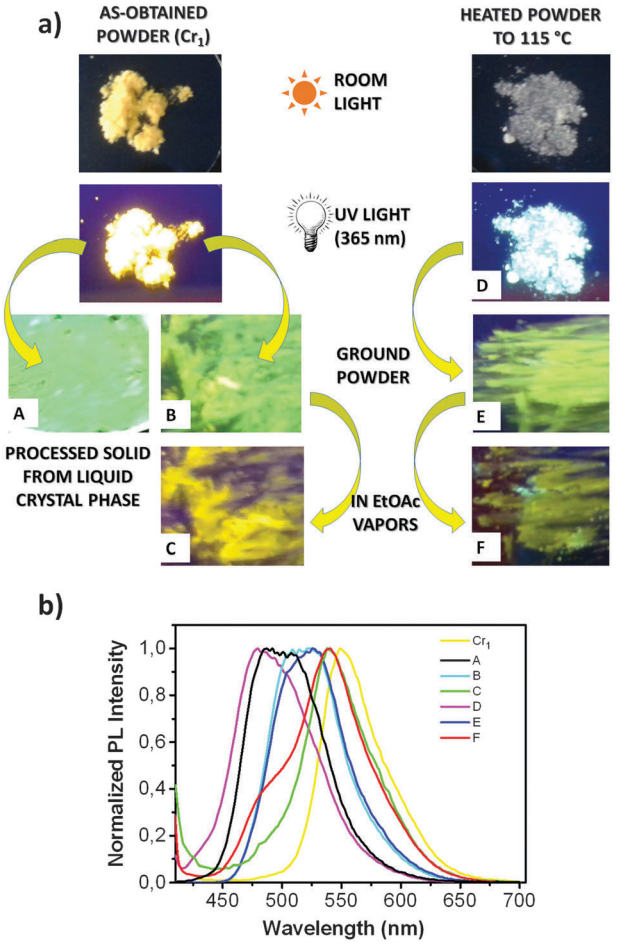

Fig. 3 (a) Thermochromism, mecanochromism and vapochromism of **DCS14** and (b) fluorescence spectra of the corresponding changes. Cr_1 (as-obtained solid), (A): processed solid by cooling down from 185 °C at r.t. at 10 °C min^{-1}. (B) After grinding Cr_1. (C) After setting B to ethyl acetate vapor. (D) Processed solid by fast cooling from 115 °C. (E) After grinding the D powder. (F) After setting E to ethyl acetate (EtOAc) vapor.

minute at 115 °C and fast cooling to room temperature yields a white powder with blue luminescence (Fig. 3D).

Mechanochromism has also been observed in **DCS14**, grinding the as-obtained powder (Cr_1) changes the luminescence from orange to yellow (Fig. 3B), or grinding the white powder (D) shifts the luminescence from blue to yellow (Fig. 3E). Finally, by exposing the ground solids (B or E) to ethyl acetate vapor the fluorescence emission reverts back nearly to the emission color of the as obtained solid (Cr_1) (Fig. 3C and F).

Photochemical properties

Aforementioned, during the synthesis, DCS derivatives undergo *Z*/*E* photoisomerization under ambient light. In order to confirm their photochemical activity, all the compounds were investigated in solution as well as in the condensed phases under irradiation with a 8 W 365 nm UV lamp.

The two rod-like compounds **DCS14** and **DCS4** were studied in solution under different irradiation times, and both showed similar results. Fig. 4a and b displays the ^{1}H NMR spectra

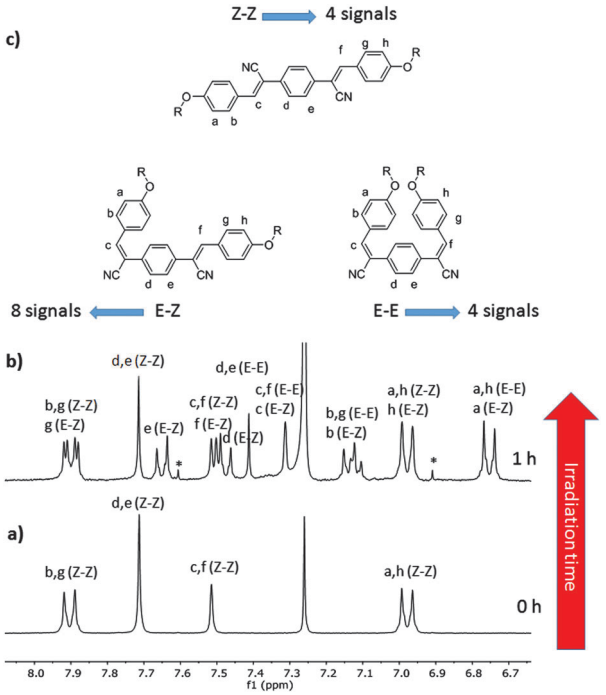

Fig. 4 Aromatic region of the ^{1}H NMR spectra of **DCS4** (a) before and (b) after irradiation of a $CDCl_3$ solution with a 365 nm UV lamp (8 W, 1 h). (c) Isomers of **DCS4** and lettering for NMR assignment.

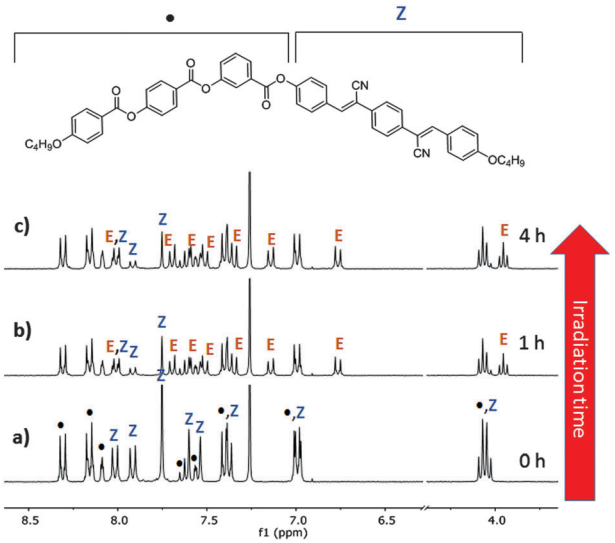

Fig. 5 Partial ^{1}H NMR spectra of **B4-DCS4** (a) before and (b) after irradiation of a $CDCl_3$ solution with a 365 nm UV lamp (8 W) for 1 h and (c) for 4 h. *Z* signals correspond to the starting estereoisomer and *E* signals appear after irradiation.

obtained for **DCS4** before and after the irradiation of a $CDCl_3$ solution for 1 hour. The appearance of new peaks at higher field corresponding to the formation of photoproducts can be observed. By DOSY experiments only a single diffusion coefficient was obtained and by mass spectra experiments only one peak of the same mass as the starting compound could be detected. This supports the *Z*/*E* photoisomerization of the –C=C(CN)-groups. However, as the compound possesses two photoisomerizable double bonds, the starting material in configuration *Z*,*Z* can give rise to two different photoproducts, *E*,*Z* and *E*,*E*-isomers (Fig. 4c). By an analysis of the ^{1}H NMR spectra and COSY experiments the signals were assigned and it could be calculated that after irradiation for 1 hour the three isomers are present in a relationship of *Z*,*Z* : *E*,*Z* : *E*,*E* of 28 : 58 : 14.

Concerning bent-core compounds, Fig. 5 shows a representative example of the isomerization process followed by ^{1}H NMR. With increasing irradiation time, spectra of **B4-DCS4** show the appearance of new peaks at higher field. Again, the DOSY experiment confirms that the photoproducts have the same diffusion coefficient as the starting material, and the mass spectra are also similar. Therefore, the photoproducts formed are a consequence of the *Z*/*E* photoisomerization of the DCS unit. As there are two isomerizable double bonds and the molecule is not symmetric three photoproducts can be generated, *E*,*E*-, *Z*,*E*- and *E*,*Z*-isomers. Due to the complexity and the superimposed signals of the non-photoreactive part of the molecule with the DCS signals a relationship of *Z*,*Z*:*Z*,*E*:*E*,*Z*:*E*,*E* could not be calculated in these cases.

The changes that occur in solution upon irradiation with a 365 nm UV lamp of both bent-core and rod-like compounds can also be monitored by UV-Vis and fluorescence spectroscopy. The absorption maxima decreases and shifts to lower wavelength. For **DCS4** the 380 nm band decreases and shifts to 364 nm as a consequence of *Z*/*E* isomerization. Two new bands appear at 330 nm and 278 nm exhibiting an isosbestic point at 347 nm. As two new photoproducts are generated, it is quite possible that the 364 nm band and the 330 nm band correspond to the appearance of the *Z*,*E*- and *E*,*E*-isomers respectively (Fig. 6a). Changes are also visible in the fluorescence spectra after irradiation (Fig. 6b). A decrease in intensity and a slight shift towards higher emission wavelengths are observed as reported previously for DCS as models for CN-PPV polymers.[37]

For the bent-core compounds similar behavior could be observed. In these cases the new bands appear at 359 nm, 316 nm and 270 nm, blue-shifted with respect to the rod-like compounds as a consequence of the different substitution of the DCS chromophore.

Photochemistry of the DCS chromophore in bulk is important to understand not only for widening the range of applications, but also to pay attention to their manipulation in the cases in which it is necessary to avoid undesired photoreactions. None of the compounds were photoactive in bulk at room temperature. However, rod-like compounds **DCS4** and **DCS14** were unstable under UV irradiation in their liquid crystal phases. Thermogravimetric analysis shows that the compounds do not decompose at such temperatures (Fig. S8, ESI†).

Compound **DCS4** under irradiation in the N mesophase at 190 °C gives rise to photoisomerized *E*,*Z*- and *E*,*E*-products and a small percentage of the dimeric product due to a [2+2]-photocycloaddition (Fig. 7b). In contrast, after the irradiation of **DCS14** in the SmC mesophase both processes (photoisomerization and photocycloaddition) occur in similar proportion (Fig. 7c).

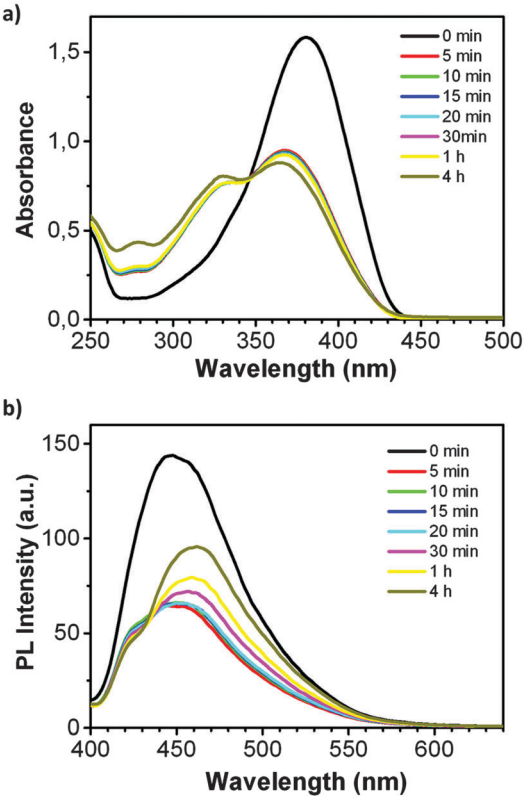

Fig. 6 (a) UV-Vis absorption spectra and (b) fluorescence spectra of **DCS4** in DCM solution under different irradiation times (365 nm, 8 W).

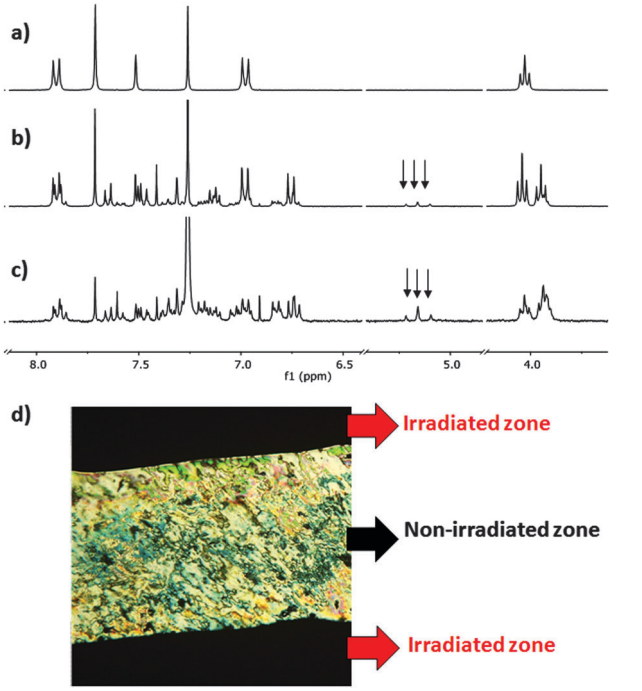

Fig. 7 Partial ^{1}H NMR spectra in $CDCl_3$ for (a) **DCS14** before irradiation (**DCS4** shows the same spectra in this region), (b) **DCS4** after irradiation in the nematic mesophase at 190 °C for 4 hours (365 nm, 8 W), (c) **DCS14** after irradiation in the smectic C mesophase at 135 °C for 4 hours (365 nm, 8 W). (d) Microphotograph between crossed polarizers of a thin film of **DCS4** irradiated in the nematic mesophase at 190 °C for 1 hour (365 nm, 8 W) through a mask showing black regions in the irradiated area (red arrows) due to a photoinduced isotropization and the texture of the nematic phase in the non-irradiated area (black arrow).

Photocycloaddition generates cyclobutanes, which can be identified by the presence of one singlet in the ^{1}H NMR at around 5 ppm.[26] In this case three singlets are observed in that region, indicating that at least three different cyclobutanes are formed.

It is worth noticing that under similar experimental conditions, depending on the type of mesophase, different photoproducts can be formed. The SmC mesophase undergoes more cycloaddition processes than the N mesophase. This can be explained by the different molecular packing of each mesophase. In the N mesophase the molecules only have a preferential orientation, in contrast, in the lamellar SmC mesophase the molecules arrange in layers, which is more favorable for a topochemical reaction such as the [2+2]-photocycloaddition, where C=C has to be in the immediate vicinity to react.

UV irradiation in the mesophase gives rise to observable birefringence changes in these materials. The N mesophase of **DCS4** undergoes phase transition to an isotropic phase upon irradiation. This can be clearly visible upon irradiation using a mask (Fig. 7d). The photoproducts formed by irradiation disturb the liquid crystalline arrangement to such an extent that the melting point is lowered generating an isotropic liquid.

The transformation from the liquid crystalline state to the isotropic liquid or a lowering of the temperature of the liquid crystal to isotropic liquid transition was also observed while standard POM investigations without a 450 nm longpass filter. Therefore, it is important to carry out the investigations with light and heat far above the absorption of the DCS chromophore in order to keep the *Z*,*Z*-isomer pure.

Conclusions

The dicyanodistyrylbenzene (DCS) chromophore has been incorporated into bent- and rod-like structures giving rise to compounds with 2D and 1D molecular structures. The molecular geometry dramatically influences the ability to stabilize liquid crystalline phases, lacking in the bent-shaped designs. In contrast to bent-core molecules, rod-like compounds exhibit liquid crystalline behavior (smectic and/or nematic mesophases). Fluorescence properties of these materials are sensitive to external stimuli. Multiresponsive behavior has been observed as emission changes in the visible spectra are observed depending on the condensed phase or stimuli, such as temperature, pressure, solvent vapor as well as photoirradiation.

All compounds undergo *Z*/*E* photoisomerization in solution under UV irradiation with relatively low power lamp sources or ambient light. In addition, photochemical activity in bulk has also been investigated, which is unprecedented in these derivatives. The crystal phase is stable towards photoirradiation while the liquid crystal phases are photoreactive giving rise to *Z*/*E* photoisomerization and [2+2]-photocycloaddition reactions.

The cycloaddition process is favored in the smectic mesophase due to the more compact lamellar packing. As a consequence of the photochemistry in bulk, a photoinduced phase transition leading to a lowering of the isotropization temperature can be observed by irradiation in the liquid crystal phase.

DCS compounds are unstable in solution or in liquid crystal phases under irradiation with UV light and also under ambient light. Therefore, aspects related to the synthesis, purification and investigation of their optical/photophysical properties should be carefully undertaken in order to obtain reproducible results and future implementation in devices based on these chromophores.

In conclusion, this study sets DCS-based liquid crystals as novel types of photoreactive materials.

Acknowledgements

The authors from ICMA greatly appreciate the financial support from the Spanish Government (MINECO-FEDER project MAT2012-38538-C03-01), the Gobierno de Aragón and FSE (project E04) and the Jae PreDoc-CSIC (M. M.-A.) fellowship program. Thanks are given also to Nuclear Magnetic Resonance, Mass Spectra and Thermal Analysis Services from the Instituto de Ciencia de Materiales de Aragón (Univ. Zaragoza–CSIC). We thank J. Gierschner (IMDEA-Nanoscience, Madrid) for access to the steady-state and time-resolved fluorescence setup, and H. Bolink (Univ. Valencia) for access to the integrating sphere.

References

1 D. Oelkrug, A. Tompert, H. J. Egelhaaf, M. Hanack, E. Steinhuber, M. Hohloch, H. Meier and U. Stalmach, *Synth. Met.*, 1996, **83**, 231–237.
2 D. Oelkrug, A. Tompert, J. Gierschner, H. J. Egelhaaf, M. Hanack, M. Hohloch and E. Steinhuber, *J. Phys. Chem. B*, 1998, **102**, 1902–1907.
3 J. Gierschner and S. Y. Park, *J. Mater. Chem. C*, 2013, **1**, 5818–5832.
4 B.-K. An, J. Gierschner and S. Y. Park, *Acc. Chem. Res.*, 2012, **45**, 544–554.
5 L. Zhu and Y. Zhao, *J. Mater. Chem. C*, 2013, **1**, 1059–1065.
6 J. Kunzelman, M. Kinami, B. R. Crenshaw, J. D. Protasiewicz and C. Weder, *Adv. Mater.*, 2008, **20**, 119–122.
7 S.-J. Yoon, J. W. Chung, J. Gierschner, K. S. Kim, M.-G. Choi, D. Kim and S. Y. Park, *J. Am. Chem. Soc.*, 2010, **132**, 13675–13683.
8 S. J. Yoon and S. Park, *J. Mater. Chem.*, 2011, **21**, 8338–8346.
9 M. S. Kwon, J. Gierschner, S.-J. Yoon and S. Y. Park, *Adv. Mater.*, 2012, **24**, 5487–5492.
10 M. S. Kwon, J. Gierschner, J. Seo and S. Y. Park, *J. Mater. Chem. C*, 2014, **2**, 2552–2557.
11 H. Lu, S. Zhang, A. Ding, M. Yuan, G. Zhang, W. Xu, G. Zhang, X. Wang, L. Qiu and J. Yang, *New J. Chem.*, 2014, **38**, 3429–3433.
12 H. J. Kim, D. R. Whang, J. Gierschner, C. H. Lee and S. Y. Park, *Angew. Chem., Int. Ed.*, 2015, **54**, 4330–4333.
13 S. Jeon, J. P. Lee and J.-M. Kim, *J. Mater. Chem. C*, 2015, **3**, 2732–2736.
14 S. J. K. Pond, M. Rumi, M. D. Levin, T. C. Parker, D. Beljonne, M. W. Day, J.-L. Brédas, S. R. Marder and J. W. Perry, *J. Phys. Chem. A*, 2002, **106**, 11470–11480.
15 W. Xie, Y. Li, F. Li, F. Shen and Y. Ma, *Appl. Phys. Lett.*, 2007, **90**, 141110.
16 H. Wang, F. Li, I. Ravia, B. Gao, Y. Li, V. Medvedev, H. Sun, N. Tessler and Y. Ma, *Adv. Funct. Mater.*, 2011, **21**, 3770–3777.
17 Y. Xu, H. Zhang, F. Li, F. Shen, H. Wang, X. Li, Y. Yu and Y. Ma, *J. Mater. Chem.*, 2012, **22**, 1592–1597.
18 S. Varghese, S. J. Yoon, E. M. Calzado, S. Casado, P. G. Boj, M. A. Díaz-García, R. Resel, R. Fischer, B. Milián-Medina, R. Wannemacher, S. Y. Park and J. Gierschner, *Adv. Mater.*, 2012, **24**, 6473–6478.
19 S. J. Yoon, S. Varghese, S. K. Park, R. Wannemacher, J. Gierschner and S. Y. Park, *Adv. Opt. Mater.*, 2013, **1**, 232–237.
20 S. M. Morris, M. M. Qasim, D. J. Gardiner, P. J. W. Hands, F. Castles, G. Tu, W. T. S. Huck, R. H. Friend and H. J. Coles, *Opt. Mater.*, 2013, **35**, 837–842.
21 S. Varghese, S. K. Park, S. Casado, R. C. Fischer, R. Resel, B. Milián-Medina, R. Wannemacher, S. Y. Park and J. Gierschner, *J. Phys. Chem. Lett.*, 2013, **4**, 1597–1602.
22 S.-J. Yoon, J. H. Kim, K. S. Kim, J. W. Chung, B. Heinrich, F. Mathevet, P. Kim, B. Donnio, A.-J. Attias, D. Kim and S. Y. Park, *Adv. Funct. Mater.*, 2012, **22**, 61–69.
23 R. Wei, Y. He, X. Wang and P. Keller, *Macromol. Rapid Commun.*, 2014, **35**, 1571–1577.
24 C. M. L. Vande Velde, F. Blockhuys, C. Van Alsenoy, A. T. H. Lenstra and H. J. Geise, *J. Chem. Soc., Perkin Trans. 2*, 2002, 1345–1351.
25 A. Gulino, F. Lupo, G. G. Condorelli, M. E. Fragala, M. E. Amato and G. Scarlata, *J. Mater. Chem.*, 2008, **18**, 5011–5018.
26 J. W. Chung, Y. You, H. S. Huh, B.-K. An, S.-J. Yoon, S. H. Kim, S. W. Lee and S. Y. Park, *J. Am. Chem. Soc.*, 2009, **131**, 8163–8172.
27 L. L. Zhu, X. Li, F.-Y. Ji, X. Ma, Q.-C. Wang and H. Tian, *Langmuir*, 2009, **25**, 3482–3486.
28 L.-L. Zhu, D.-H. Qu, D. Zhang, Z.-F. Chen, Q.-C. Wang and H. Tian, *Tetrahedron*, 2010, **66**, 1254–1260.
29 L. Zhu, C. Y. Ang, X. Li, N. Kim Truc, S. Y. Tan, H. Agren and Y. Zhao, *Adv. Mater.*, 2012, **24**, 4020–4024.
30 L. Zhu, X. Li, Q. Zhang, X. Ma, M. Li, H. Hang, Z. Luo, H. Agren and Y. Zhao, *J. Am. Chem. Soc.*, 2013, **135**, 5175–5182.
31 J. W. Chung, S.-J. Yoon, B.-K. An and S. Y. Park, *J. Phys. Chem. C*, 2013, **117**, 11285–11291.
32 H. Lu, L. Qiu, G. Zhang, A. Ding, W. Xu, G. Zhang, X. Wang, L. Kong, Y. Tian and J. Yang, *J. Mater. Chem. C*, 2014, **2**, 1386–1389.
33 J. Seo, J. Chung, J. E. Kwon and S. Park, *Chem. Sci.*, 2014, **5**, 4845–4850.
34 J. W. Park, S. Nagano, S.-J. Yoon, T. Dohi, J. Seo, T. Seki and S. Y. Park, *Adv. Mater.*, 2014, **26**, 1354–1359.

35 Y. Jin, Y. Xia, S. Wang, L. Yan, Y. Zhou, J. Fan and B. Song, *Soft Matter*, 2015, **11**, 798–805.
36 P. Xing, H. Chen, L. Bai and Y. Zhao, *Chem. Commun.*, 2015, **51**, 9309–9312.
37 F. J. Lange, M. Leuze and M. Hanack, *J. Phys. Org. Chem.*, 2001, **14**, 474–480.
38 Y. Li, H. Xu, L. Wu, F. He, F. Shen, L. Liu, B. Yang and Y. Ma, *J. Polym. Sci., Part B: Polym. Phys.*, 2008, **46**, 1105–1113.
39 P. Duan, N. Yanai, Y. Kurashige and N. Kimizuka, *Angew. Chem., Int. Ed.*, 2015, **54**, 7544–7549.
40 M. Martínez-Abadía, B. Robles-Hernández, B. Villacampa, M. R. De La Fuente, R. Giménez and M. B. Ros, *J. Mater. Chem. C*, 2015, **3**, 3038–3048.
41 M. Martínez-Abadía, S. Varghese, B. Milián-Medina, J. Gierschner, R. Giménez and M. B. Ros, *Phys. Chem. Chem. Phys.*, 2015, **17**, 11715–11724.
42 M. J. Holm, F. B. Zienty and M. A. Terpstra, *J. Chem. Eng. Data*, 1968, **13**, 70–74.
43 N. Gimeno and M. Blanca Ros, in *Handbook of Liquid Crystals*, ed. J. W. Goodby, P. J. Collings, T. Kato, C. Tschierske, H. Gleeson and P. Raynes, Wiley-VCH, Weinheim, 2014, vol. 4, pp. 603–739.
44 S.-J. Yoon, J. H. Kim, J. W. Chung and S. Y. Park, *J. Mater. Chem.*, 2011, **21**, 18971–18973.
45 J. Gierschner, L. Lüer, B. Milián-Medina, D. Oelkrug and H.-J. Egelhaaf, *J. Phys. Chem. Lett.*, 2013, **4**, 2686–2697.